Journal of Medicinal Chemistry

Article

pubs.acs.org/jmc

Pyrimethamine Derivatives: Insight into Binding Mechanism and Improved Enhancement of Mutant β-*N*-acetylhexosaminidase Activity

Michael B. Tropak,[†] Jianmin Zhang,[‡] Sayuri Yonekawa,[†] Brigitte A. Rigat,[†] Virender S. Aulakh,[‡] Matthew R. Smith,[‡] Hee-Jong Hwang,[‡] Marco A. Ciufolini,[‡] and Don J. Mahuran*[,†,§]

[†]Genetics and Genome Biology, SickKids, PGCRL 686 Bay Street, Toronto, Ontario M5G 0A4, Canada

[‡]Department of Chemistry, University of British Columbia, 2036 Main Mall Vancouver, British Columbia V6T 1Z1, Canada

[§]Department of Laboratory Medicine and Pathology, University of Toronto, Medical Science Building, 1 King's College Circle, 6th Floor, Toronto, Ontario M5S 1A8, Canada

Supporting Information

ABSTRACT: In order to identify structural features of pyrimethamine (5-(4-chlorophenyl)-6-ethylpyrimidine-2,4-diamine) that contribute to its inhibitory activity (IC_{50} value) and chaperoning efficacy toward β-*N*-acetylhexosaminidase, derivatives of the compound were synthesized that differ at the positions bearing the amino, ethyl, and chloro groups. Whereas the amino groups proved to be critical to its inhibitory activity, a variety of substitutions at the chloro position only increased its IC_{50} by 2−3-fold. Replacing the ethyl group at the 6-position with butyl or methyl groups increased IC_{50} more than 10-fold. Surprisingly, despite its higher IC_{50}, a derivative lacking the chlorine atom in the *para*-position was found to enhance enzyme activity in live patient cells a further 25% at concentrations >100 μM, while showing less toxicity. These findings demonstrate the importance of the phenyl group in modulating the chaperoning efficacy and toxicity profile of the derivatives.

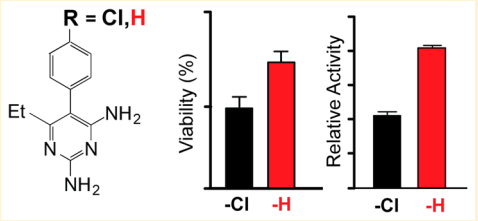

INTRODUCTION

Pyrimethamine (PYR, **1**, Figure 1A) is a known human antimalarial drug that inhibits the parasite's (e.g., *Plasmodium falciparum*) dihydrofolate reductase (DHFR).[1] Interestingly, the compound also acts as an effective pharmacological chaperone (PC) for lysosomal β-*N*-acetylhexosaminidase A (Hex A).[2] Indeed, we have shown that, in some late-onset forms of GM2 gangliosidosis (Tay-Sachs and Sandhoff diseases), the Hex A activity in patient fibroblasts can be enhanced by 2−3-fold.[3] Recently it has been reported that treating Dutch APP^{E693Q} mice (a mouse model of Alzheimer's disease) with a PC for Hex dramatically reduced the accumulation of a β-amyloid peptide:ganglioside (GM2 and GM3) complex. This reduction was associated with improved learning behavior and decreased anxiety in the treated mice.[4] Thus, PCs of Hex have the potential to treat a much broader patient base than just those with late-onset Tay-Sachs or Sandhoff disease.

Three Hex isozymes arise through the combinatorial dimerization of two subunits encoded by two evolutionarily related genes, the α (encoded by the *HEXA* gene) and/or β (*HEXB* gene), i.e, the major Hex A (αβ) and Hex B (ββ) isozymes and the minor, unstable Hex S (αα) isozyme.[5] Of the three Hex isozymes, only heterodimeric Hex A is able to efficiently associate with the GM2 activator protein/GM2 ganglioside (GM2) to form the ternary complex and hydrolyze the non-reducing terminal β-1,4-linked *N*-acetylgalactosamine from GM2, producing GM3 ganglioside. In the late-onset variants of GM2 gangliosidosis, point mutations in either the α-subunit (Tay-Sachs disease) or the β-subunit (Sandhoff disease)[6] reduce the activity of Hex A below a critical threshold

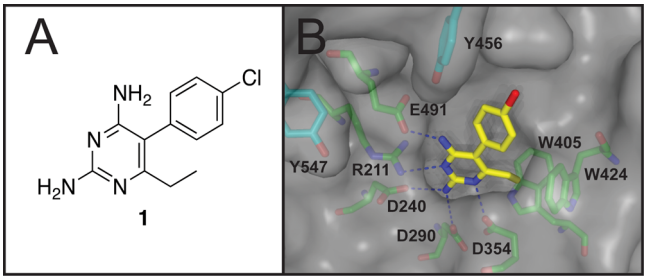

Figure 1. (A) Structure of pyrimethamine (PYR). (B) Amino acid residues (green) in the active site involved in binding PYR (yellow). The chlorine atom on PYR is highlighted in red. Residues participating in formation of the active site from the adjacent subunit are shown in marine blue. Amino acid residues (D290, D240, E491) directly forming hydrogen bonds (denoted with dashed blue lines) with the amino (blue) groups on PYR are highlighted in green. The ethyl group of PYR is found in a hydrophobic pocket formed by residues W405 and W424 (green).

Received: November 27, 2014
Published: May 18, 2015

ACS Publications © 2015 American Chemical Society

DOI: 10.1021/jm5017895
J. Med. Chem. 2015, 58, 4483−4493

of enzyme activity needed to prevent GM2 storage (5−10% of normal values).[7] Since PYR is a micromolar inhibitor of Hex isozymes (inhibitory activity (IC_{50}) = 15 μM), it binds to and stabilizes the folded mutant enzyme in the endoplasmic reticulum (ER), thereby increasing the number of molecules that are able to retain their active folded conformation, allowing the proper disulfide bonds to form and the enzyme to be transported to the lysosome.[2] The presence of disulfide bonds, the acidic pH of the lysosome, and the presence of substrate all combine to displace PYR while continuing to stabilize Hex A. Additionally, the K_i of PYR as an inhibitor of Hex increases at acidic pH.

We have demonstrated experimentally that PYR treatment of late-onset Tay-Sachs patients' cells loaded with a fluorescent GM2 ganglioside analogue produces an enhancement of the cells' ability to turnover the substrate.[8] However, the chaperoning efficacy of PYR is mutation dependent.[2]

The structure of Hex B in complex with PYR has only recently been elucidated.[9] Amino acids Asp240 and Glu491 are within hydrogen-bonding distances of the amino groups in PYR and are predicted to act as hydrogen bond acceptors (Figure 1B). The ethyl group of PYR is positioned within a hydrophobic pocket formed by Trp405, Trp424, and Trp489. The chlorine atom in the *para*-position on the phenyl of PYR forms a weak hydrogen bond with a conserved water molecule near the mouth of the substrate-binding pocket and points toward the bulk solvent.

PYR has been evaluated in both adult-onset Tay-Sachs disease (ATSD) and Sandhoff disease (ASD) patients in an open-label Phase I/II clinical trial to evaluate treatment efficacy and tolerability.[3] The observed increase in Hex A activity levels in patients' leukocytes (up to a maximum of 4-fold) was closely correlated with their plasma levels of PYR, which varied according to the oral dose of the drug (25, 50, 75, or 100 mg/day) and the metabolism of each patient; i.e., patients taking the same dose could have very different levels of plasma PYR. As an anti-malarial, PYR has 1000-fold higher affinity for the parasite versus human DHFR. Patients in this study were supplemented with folic acid (leucovorin) as a precaution against human DHFR inhibition. Nonetheless, side effects were seen in most patients treated with PYR at or above 75 mg or with plasma levels >1.5 mg/L. Therefore, it would be desirable to obtain derivatives of PYR that enhance Hex activity while concomittantly minimizing undesirable side effects.

In order to identify features of PYR that contribute to its Hex inhibitory activity and chaperoning efficacy, i.e., PC activity, as well as possibly contributing to the detrimental side effects seen at higher doses, derivatives of the compound were synthesized. These differed from PYR at the positions bearing the amino, ethyl, and chloro groups. Whereas the amino groups and the ethyl group at the 5-position proved to be critical for its PC activity, a variety of substitutions at the chloro position only increased the IC_{50} by 2−3-fold. Surprisingly, the derivatives lacking the pendant chloro group were found to enhance enzyme activity in live patient cells by a further 25% at concentrations >100 μM, despite their higher IC_{50}. Combined with the 3D structure of the Hex A, these derivatives have provided additional insight into the binding mechanism of PYR, as well as into features associated with improved chaperoning efficacy and reduced toxicity.

RESULTS AND DISCUSSION

To gain insight into the molecular details of how PYR binds to Hex, and to identify PYR derivatives with improved enzyme enhancement efficacy in terms of dosing and response, three regions of **1** (PYR) were modified: (1) the 2,4-diamino groups on the pyrimidine backbone, (2) the 6-ethyl alkyl side chain, and (3) the phenyl group itself or the substituents on the phenyl group attached to the pyrimidine ring.

Synthesis of PYR Analogues. Analogues of PYR retaining the 2,4-diaminopyrimidine motif were prepared according to published procedures[10] as outlined in Scheme 1, which also lists

Scheme 1. General Procedure for Synthesis of PYR Analogues and Representative Compounds Examined in This Study

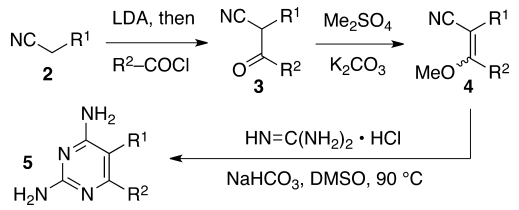

compound	R^1	R^2	compound	R^1	R^2
5a	4-Cl-C_6H_4	Me	**5g**	4-CF_3-C_6H_4	Et
5b	4-Cl-C_6H_4	*n*-Pr	**5h**	Ph	Et
5c	4-Cl-C_6H_4	*i*-Pr	**5i**	4-Me-C_6H_4	Et
5d	4-Cl-C_6H_4	*n*-Bu	**5j**	3-Me-C_6H_4	Et
5e	4-Cl-C_6H_4	CH_2NH_2	**5k**	2-Me-C_6H_4	Et
5f	4-MeO-C_6H_4	Et	**5l**	3,5-di-Me-C_6H_3	Et

the structures of representative compounds examined in the course of this study. Deaminated variants of **1** and **5g** were obtained starting with vigorous acid hydrolysis of the parent compounds,[11] followed by reaction of the emerging pyrimidinones with $POCl_3$ and hydrogenolysis of the resultant chloropyrimidines (Scheme 2). Pyrimidines such as **11** were prepared in a like fashion from compounds of the type **10**, which in turn were obtained by reaction of an appropriately substituted compound **4** with urea in EtOH−EtONa.[11]

Inhibitory Activity of the Deaminated Analogues of PYR. Enzyme activity of purified human Hex A in the presence of the different PYR analogues was monitored using the

Scheme 2. Preparation of Des-amino Analogues of 1 and 5g

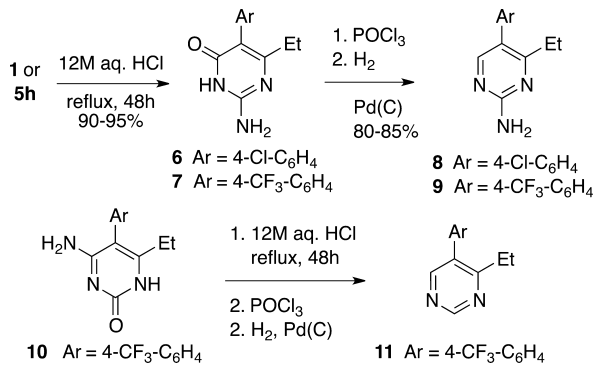

DOI: 10.1021/jm5017895
J. Med. Chem. 2015, 58, 4483−4493

colorimetric substrate *p*-nitrophenyl-β-D-*N*-acetylglucopyranoside (pNPGlcNAc) (see Experimental Section). Removal of one (cf. **8**, **9**) or both (cf. **11**) amino groups from the pyrimidine ring resulted in a >10-fold increase in IC_{50} values (Table 1). Substitution of the 4-amino group with a carbonyl (cf. **6**) also resulted in a >120-fold increase in IC_{50}. Both amino groups are therefore essential for activity. This is consistent with their role as H-bond donors within the active site of the enzyme deduced from the 3D structure of the HexB:PYR complex.[9]

Table 1. Biological Activities of Some Des-amino PYR Analogues

	compound				
	1	**6**	**8**	**9**	**11**
IC_{50}[a]	17 ± 3	>2100	>400	>400	>940
PC activity[b]	2.1 ± 0.1	–	–	–	–

[a]IC_{50} (μM) determined using purified human Hex A and pNPGlcNAc (0.5 mM). [b]PC activity: Intracellular enhancement (increase in) of enzyme activity based on the ratio of Hex A activity in treated ATSD patient fibroblasts versus mock treated (DMSO). Enzyme activity was based on the hydrolysis of the α-active-site specific MUGS (1.6 mM) by lysates from treated and untreated ATSD patient fibroblasts.

Inhibitory Activity of PYR Analogues with Modified 6-Alkyl Side Chains. Shortening of the alkyl side chain from an ethyl to methyl side arm resulted in a more than 25-fold increase in IC_{50} values, i.e., from 17 to 560 μM (Table 2).

Table 2. Effect of the Side-Chain Length on the Biological Activity of PYR Analogues 5

compd	R^1	R^2	IC_{50}[a]	PC activity[b]
1	4-Cl-C_6H_4	Et	17 ± 3	2.1 ± 0.1
5a	4-Cl-C_6H_4	Me	>560	–
5b	4-Cl-C_6H_4	*n*-Pr	18 ± 3	1.5 ± 0.1
5c	4-Cl-C_6H_4	*i*-Pr	>410	–
5d	4-Cl-C_6H_4	*n*-Bu	>1400	–
5e	4-Cl-C_6H_4	CH_2NH_2	180 ± 20	–

[a]IC_{50} (μM): see Table 1, footnote *a*. [b]PC activity: see Table 1, footnote *b*.

Similarly, increasing the length beyond a propyl or introducing a branched chain, such as isopropyl, also resulted in a more than 20-fold increase in IC_{50} values relative to PYR. By comparison, the IC_{50} of the propyl derivative was not significantly different than that of PYR. These results are in line with the size of a hydrophobic pocket formed by Trp residues 405, 424, and 489 that can, in the context of a 6-alkyl side chain on PYR, accommodate an ethyl or propyl but not a bulkier group, such as butyl or isopropyl.[9,12] A similar trend in increasing IC_{50} was observed with thiazoline derivatives that contained analogously positioned alkyl chains of increasing size.[13]

The general acid−base residue of Hex B (Glu355) is located near the hydrophobic pocket, and its proximity suggested that replacing the alkyl side chain with an amino group would improve binding via formation of an additional electrostatic interaction. However, substitution of the 6-ethyl group with methylamine resulted in a >10-fold increase in the IC_{50}, whereas replacement with an azidomethyl group did not significantly affect the IC_{50} value.

Inhibitory Activity of PYR Analogues with Modified Aryl Groups. Bateman et al. in 2011 demonstrated that the chlorine atom on the phenyl group makes a hydrogen bond with a water molecule located near the entrance to the active site of Hex; however, the phenyl ring was found to project toward the bulk solvent, suggesting that a larger variety of substitutions could be accommodated on the underlying ring without greatly affecting its binding affinity toward the enzyme.[9] Several PYR derivatives, differing in terms of the pendant group (chloro, methyl, methoxy, or trifluoromethyl) and their relative position (*meta*, *para*, or *ortho*) on the phenyl ring, were synthesized and evaluated for inhibitory activity and chaperoning efficacy. Representative examples are shown in Table 3. Derivatives incorporating a *para*-substituted phenyl group (**5f**, **5g**, and **5i**), irrespective of the nature of the substituent, displayed an average IC_{50} value (24 ± 13 μM) similar to that of PYR (17 ± 3 μM). Collectively, this group of compounds, including PYR, will be referred to as the PYR analogues bearing a *para*-substituted phenyl group. In contrast, analogues containing an *ortho*- or *meta*-substituted phenyl group (**5j**, **5k**, **5l**) and/or lacking a substituent in the *para*-position (**5h**) on average showed a 2.4-fold higher IC_{50} (41 ± 5 μM) compared to PYR. Collectively, this group of compounds is referred to as the PYR analogues lacking a *para*-substituted phenyl group. The increased IC_{50} values associated with this group of compounds may reflect the steric clashes of *ortho*- and *meta*-positioned pendant groups with the residues at the entrance to the active site, due to the of axial rotation of the phenyl group. Such steric clashes would be minimized in the *para*-positioned PYR analogues.

Table 3. Effect of Phenyl Group Substitution on the Biological Activity of PYR Analogues 5

compd	R^1	R^2	IC_{50}[a]	PC activity[a]
1	4-Cl-C_6H_4	Et	17 ± 3	2.1 ± 0.1
5f	4-MeO-C_6H_4	Et	18 ± 6	2.0 ± 0.3
5g	4-CF_3-C_6H_4	Et	15 ± 2	2.2 ± 0.1
5h	Ph	Et	32 ± 5	2.7 ± 0.1
5i	4-Me-C_6H_4	Et	40 ± 16	1.7 ± 0.1
5j	3-Me-C_6H_4	Et	34 ± 7	2.9 ± 0.1
5k	2-Me-C_6H_4	Et	43 ± 4	2.3 ± 0.1
5l	3,5-di-Me-C_6H_4	Et	47 ± 6	2.5 ± 0.1

[a]IC_{50} (μM): see Table 1, footnote *a*. [b]PC activity: see Table 1, footnote *b*.

Chaperoning Efficacy of PYR Derivatives. To compare the enzyme enhancement efficacy of the PYR derivatives in Tables 2 and 3, fibroblasts from a patient with ATSD were treated for 5 days with the different PYR derivatives. Only compounds with an IC_{50} value of less than 100 μM were evaluated. Although the IC_{50} values of PYR and **5b** differed by less than 20%, they diverged significantly in their ability to enhance mutant (G269S) Hex A activity in ATSD patient fibroblasts. Whereas PYR treatment resulted in a maximal increase of 2.1-fold in Hex A activity, the larger propyl derivative (**5b**) showed only a 1.5-fold increase, a relative decrease of 35% in chaperoning efficacy. This underscores the importance of the size of the 6-alkyl chain, and given its importance in binding, it is unlikely that any further modifications of this group would lead to an improved level of enhancement. On the other hand, the relatively minor effect on IC_{50} values (approximately 2−3-fold increase) associated

DOI: 10.1021/jm5017895
J. Med. Chem. 2015, 58, 4483−4493

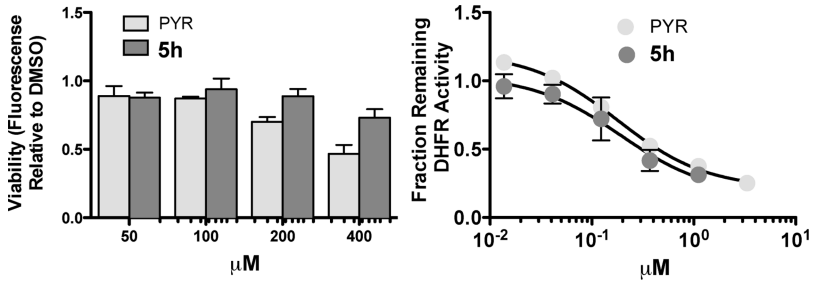

Figure 2. Comparison of the toxicity of PYR and **5h** in patient fibroblasts and their respective *in vitro* inhibitory activity against human DHFR.

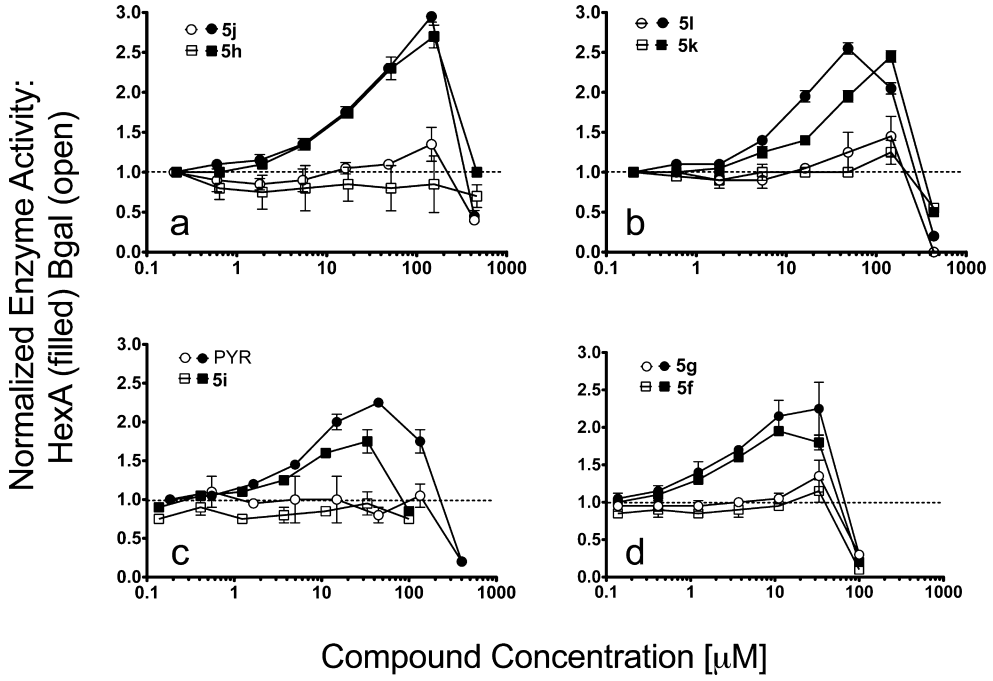

Figure 3. Comparison of *in cellulo* enhancement of mutant Hex A enzyme activity in ATSD fibroblasts by selected PYR derivatives bearing modifications on the 5-phenyl group at various concentrations, i.e., determination of the level of "maximal increase" for each derivative. Panels (a) **5j**, circles, and **5h**, squares; (b) **5l**, circles, and **5k**, squares; (c) PYR, circles, and **5i**, squares; and (d) **5g**, circles, and **5f**, squares, all giving the graphical representations of the dose−response curves. Open symbols represent the *β*-galactosidase (Bgal) activity ratio, which serves as a control for toxicity, e.g., open circles, for each drug, and the same filled symbols, e.g., filled circles, represent the Hex A activity ratio between treated and mock treated cells.

with changing the pendant group linked to the 5-phenyl ring alludes to the potential for increasing the chaperoning potency of the PYR derivatives by modifying the aryl group.

Chaperoning Efficacy of PYR Analogues Bearing a Modified Aryl Group. The group of PYR analogues **bearing** a pendant group in the *para*-position on the phenyl ring (Table 3: **5f**, **5g**, and **5i**) enhanced intracellular mutant Hex A activity in ATSD patient fibroblasts (2.0 ± 0.3-fold average enhancement) to a similar degree as PYR (2.1 ± 0.1-fold). In contrast, the PYR derivatives **lacking** a pendant group in the *para*-position (**5j**, **5k**, **5l**, and **5h**) on average enhanced intracellular Hex A activity to a greater degree (30% higher values, i.e., 2.6 ± 0.3-fold enhancement) than either PYR (2.1 ± 0.1-fold) or the derivatives incorporating a *para*-substituted phenyl group (2.0 ± 0.3-fold). These results demonstrated that derivatives **lacking** a substituent at the *para*-position on the phenyl moiety generally showed an enhanced ability to increase the intracellular activity of mutant Hex A in ATSD patients, despite having decreased inhibitory activities (higher IC_{50}) compared to PYR. Compounds **5h** and **5j** produced the greatest maximal increase in mutant Hex A activity in ATSD patient fibroblasts: 2.7- and 2.9-fold, respectively. Among the three, treatment with compound **5h** demonstrated the least decline in cell viability at the highest concentration employed. The decreased toxicity of **5h** compared to PYR was confirmed using the Alamar blue assay as an independent readout of cell viability (Figure 2). Additionally, the nearly identical IC_{50} values of the two compounds for human DHFR argue against attributing the disparity in toxicity profiles to their differences in inhibitory activity for the human enzyme. As an alternative target to account for the differential toxicity of PYR and **5h**, it is interesting to note that PYR is known to significantly decrease phosphorylation of STAT3, which is necessary for its activation.[14] Furthermore, decreased phosphorylation of STAT3 is observed in cells treated with 100 μM PYR. Although these effects were observed in different cells, the concentrations at which these observations were made are very similar to the concentrations (30−100 μM) at which significant toxicity was seen in PYR-treated patient fibroblasts. Activation of STAT3 is required for cell proliferation and cell survival.[15,16]

DOI: 10.1021/jm5017895
J. Med. Chem. 2015, 58, 4483−4493

Table 4. Inhibitory Activity of PYR and 5h for Different Hex Isozymes at Acidic and Neutral pH

	pH 4.5		pH 4.5		pH 7.0	
compd	Hex A[a]	Hex B[a]	Hex A[b] WT	Hex A[b] G269S	Hex A[a]	Hex B[a]
1	8.9 ± 1.1[c]	9.1 ± 1.2	14 ± 4	8.5 ± 3.0	3.1 ± 1.0	4.5 ± 1.2
5h	30 ± 3	38 ± 5	27 ± 5	27 ± 6	11 ± 2	15 ± 3

[a]Hex isozymes were purified from human placenta. [b]The Hex A isozyme, wild-type (WT), or mutant (G269S) was isolated from lysates of normal or ATSD fibroblasts, respectively, by ion exchange chromatography. [c]All IC_{50s} (μM) were determined using the universal MUG (1.6 mM) Hex substrate.

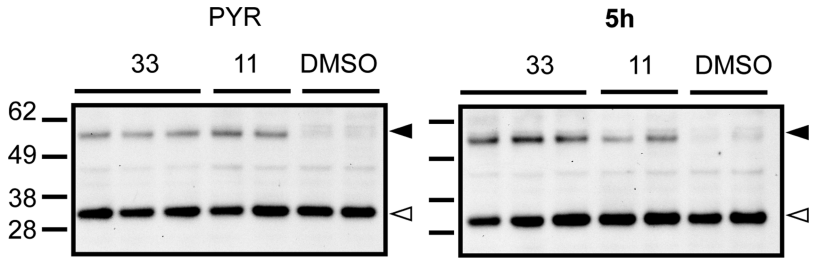

Figure 4. Steady-state protein levels of the Hex α-subunit are increased to a greater degree in **5h**- versus PYR-treated patient fibroblasts. Lysates from ATSD patient fibroblasts were treated for 5 days with PYR (33 or 11 μg/mL) or **5h** (33 or 11 μg/mL) and analyzed by Western blotting using a proprietary rabbit polyclonal IgG against human Hex A, followed by anti-rabbit peroxidase conjugated IgG and chemiluminescence detection (ECL kit, Amersham). Solid and open arrowheads denote position of bands corresponding to the mature (lysosomal) α- and β-subunits of Hex, respectively.

One could speculate that differential effects of PYR and **5h** on the phosphorylation of STAT3 could account for the variations in the toxicity profiles of the two compounds. Irrespective of the mechanism of action in terms of toxicity, the fact remains that **5h** appears to be significantly less toxic than PYR, and that this decrease in toxicity likely accounts for the increased chaperoning efficacy of **5h** at higher concentrations. Therefore, **5h** and PYR were compared in terms of their effects on intracellular trafficking of Hex A and *in cellulo* hydrolysis of a GM2 ganglioside derivative at the concentrations that corresponded to each compound's highest level of chaperone efficacy. A closer examination of the enzyme enhancement capability of the phenyl derivatives over a range of treatment concentrations (Figure 3) revealed that the peak increase occurs at a 2−3-fold lower concentration (30−40 μM) for the *para*-positioned functional groups as compared to those analogues functionalized at other positions (100−140 μM). This treatment range parallels the differences seen in the IC_{50} values between the two classes of analogues (i.e., those **bearing** versus those **lacking** a *para*-substitution on the phenyl ring).

The activity level of another lysosomal enzyme (β-galactosidase), which is not inhibited by PYR or its derivatives, was used as a surrogate marker of cell viability. At the highest concentration evaluated (>400 μM), all PYR derivatives, including the parent compound but excluding **5h**, showed a >60% reduction in β-galactosidase activity, indicative of decreased cell viability. The *para* class of derivatives exemplified by PYR showed significant signs of declining viability at lower concentrations (<200 μM) compared to the non-*para* class of compounds, such as **5h**, which showed a decline in viability at concentrations >200 μM.

Comparison of the Inhibitory Activity of PYR and 5h against Different Hex Isozymes and Wild-Type versus Mutant Hex A. As an alternative explanation for the differences in chaperoning efficacy between PYR and **5h**, it was possible that they exhibited different inhibitory activity toward wild-type versus mutant Hex A. However, their IC_{50} values for the wild-type Hex A and B isozymes were similar, differing by less than 30% (Table 4).

The inhibitory activity of **5h**, like that of PYR, also showed an approximately 2.5-fold decrease in IC_{50} values at neutral versus acidic pH. Although it is a relatively small change, both compounds would be expected to bind to the mutant enzyme to a greater degree in the neutral pH of the ER, facilitating protein folding, versus the acidic environment of the lysosome, where the complex needs to dissociate in order for the enzyme to turnover its substrate.

Comparison of Lysosomal Targeting of mutant Hex A by PYR and 5h. On the basis of protein levels observed by Western blotting (Figure 4), peak levels of mature, lysosomally derived Hex α-subunit (~55 kDa)[17] were seen in lysates from ATSD patient cells treated with 33 μg/mL of **5h** and 11 μg/mL of PYR, relative to mock (1% DMSO) treated cells. Maximal levels of mature Hex α-subunit were higher in **5h**-treated than in PYR-treated cells. The increased steady-state levels of the Hex subunit protein paralleled the increase in Hex A enzyme activity levels observed in similarly treated ATSD cells (Figure 3). These results are suggestive of increased transport of mutant Hex A to the lysosome in ATSD cells treated with **5h** compared to those treated with PYR. Immunofluorescence staining of **5h**/PYR-treated versus mock treated patient cells was used as an independent verification of increased transport of mutant Hex A to the lysosomes in the presence of either compound (Figure 5). On the basis of fluorescence intensity alone, increased levels of Hex A (green) were observed in both **5h**- and PYR-treated cells, compared to mock treated cells. Increased colocalization of signals from antibodies directed against Hex A and LAMP1, a lysosomal marker, was further evidence of increased transport of mutant Hex A to lysosomes.

Improved Hydrolysis of a Fluorescent Ganglioside Derivative in Live, PYR-Treated, or 5h-Treated Cells. Cell feeding experiments using a fluorescent GM2 ganglioside analogue were used to directly measure intralysosomal hydrolysis of GM2 ganglioside in live ATSD patient cells (i.e., an *in cellulo* assay).[8] Fibroblasts from an ATSD patient

DOI: 10.1021/jm5017895
J. Med. Chem. 2015, 58, 4483−4493

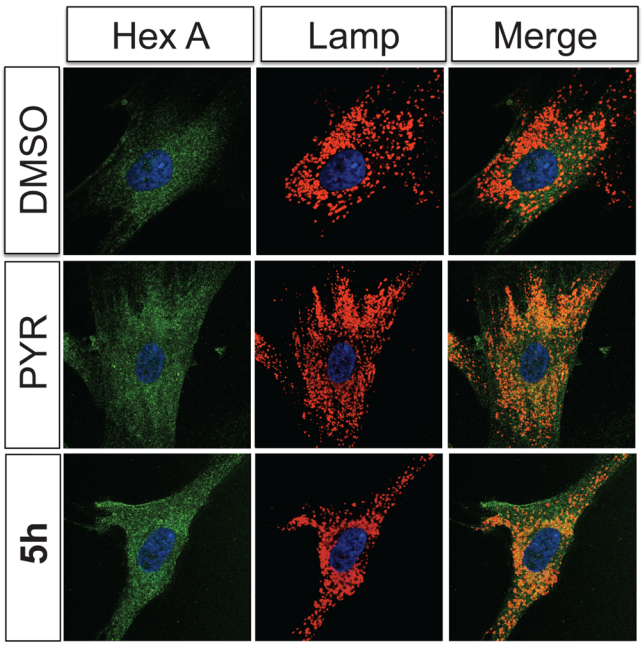

Figure 5. Increased colocalization (yellow) of Hex A (green) protein with the lysosomal marker LAMP1 (red), following the treatment of p.G269S/p.G269S α-Hex patient fibroblasts with either **5h** (33 μg/mL) or PYR (11 μg/mL). Nuclei are shown stained in blue (DAPI). Treated fibroblasts were permeabilized and probed with a proprietary rabbit polyclonal IgG anti-Hex A pre-absorbed with purified human Hex B and a LAMP1 mouse antibody. Primary antibody binding was visualized using the corresponding secondary Alexa Fluor 488 chicken anti-rabbit (green) or Alexa Fluor 594 chicken anti-mouse conjugated antibodies (red). Colocalization of Hex A and LAMP1 staining is shown on panels labeled MERGE.

were first treated with PYR (11 μg/mL) or **5h** (33 μg/mL) for 10 days to build up their levels of active mutant Hex A prior to feeding the cells with the fluorescent analogue of GM2. The doses of PYR and **5h** used to treat cells were chosen on the basis of the concentrations previously determined to produce the maximal increases in both Hex A protein and activity (MUGS) levels in treated cells, i.e., the best balance between their chaperoning versus toxicity profiles. Unlike *in vitro* assays of cell lysates with artificial colorimetric/fluorogenic substrates, *in cellulo* hydrolysis of the fluorescent GM2 occurs in the lysosomes and requires the mutant enzyme to functionally interact with the GM2 activator protein:GM2 complex. This assay also allows a read-out of any residual inhibition of Hex A caused by the chaperone once the complex enters the lysosome. Following Folch extraction of treated cells, neutral glycolipids (i.e., glycolipids produced further downstream in the GM2 breakdown pathway) in the organic phase and acidic gangliosides in the aqueous phase were resolved by high-performance thin-layer chromatography (Figure 6A). Patient cells treated with **5h** (33 μg/mL) demonstrated a greater intracellular hydrolysis of the fluorescent derivative of GM2 compared to cells treated with PYR (11 μg/mL), as indicated by the higher levels of the band corresponding to GM3. Quantification of the intensity of all bands corresponding to the downstream products of GM3 hydrolysis, lactosylceramide (LacCer) and glucosylceramide (GlcCer) (further hydrolysis was inhibited by the inclusion of an irreversible inhibitor of glucocerebrosidase in the cell feeding assay[8]), in both phases clearly shows increased levels of the products, indicative of increased lysosomal Hex A activity in response to treatment with either compound. However, **5h** treatment resulted in an additional ~1.5-fold increase in GM2 hydrolysis in comparison to that of PYR-treated cells (Figure 6B). A parallel increase is observed in Hex A activity measured in the same lysates using the fluorogenic substrate MUGS (Figure 6C). These results are significant for two reasons. First, there is always a concern that inhibitory molecules acting as PCs could continue inhibiting the activity of Hex A in the lysosome. These results clearly demonstrate that this is not the case for PYR or **5h**, as a robust increase in GM2 hydrolysis was observed, while it is very likely that, at higher concentrations of either compound, one would eventually see residual inhibition in lysosomes. However, at such higher concentrations, cellular toxicity would also become an issue. Thus, these doses represent the high end of those expected to be used to treat patients. Second, using two orthogonal Hex A enzyme assays, the results clearly and convincingly demonstrate that, at higher concentrations, **5h** is superior to PYR in enhancing lysosomal levels of Hex A activity. These results are also significant from a therapeutic perspective. Since **5h** is less toxic at higher concentrations than PYR in cells, it likely could be used at the higher doses in ATSD and ASD patients, which would further enhance Hex A activity beyond the critical threshold necessary to prevent the continuous storage of GM2 gangliosides in their lysosomes.

The therapeutic potential of **5h** is predicated on its ability to cross the blood brain barrier (BBB). Pharmacokinetic studies in small animals and quantification of drugs levels in serum and cerebrospinal fluid of PYR-treated GM2 gangliosidosis[3] and AIDS[18] patients have clearly demonstrated that PYR crosses the BBB, i.e., enters the nervous system. The physiochemical properties of PYR in terms of number of hydrogen acceptors (4) and calculated LogP (lipophilicity) value (2.8) are congruent with other drugs capable of crossing the BBB.[19] Thus, the fact that **5h** is similar to PYR with regard to number of hydrogen acceptors (4) and predicted LogP value (PYR, 2.8, versus **5h**, 2.2) suggests that **5h** would also be capable of crossing the BBB—this will need to be verified experimentally.

Recently it has been reported that treating Dutch APP^{E693Q} mice (a mouse model of Alzheimer's disease) with a PC for Hex dramatically reduced the accumulation of a β-amyloid peptide:ganglioside (GM2 and GM3) complex, improved learning behavior, and decreased anxiety.[4] Indeed, we have preliminary data demonstrating that both PCs, PYR and **5h**, are able to increase the activity levels of wild-type Hex A by approximately 1.3-fold ($p < 0.05$) relative to Hex A in DMSO-treated fibroblasts from non-GM2 gangliosidosis patients (Supporting Information, Figure 1S). Taken together with the data demonstrating the effectiveness of PYR and **5h** in enhancing mutant Hex A activity, these observations suggest that these compounds not only could be used to treat some forms of GM2 gangliosidosis but also could be potential therapeutics for Alzheimer's disease.

■ CONCLUSION

We have experimentally verified the importance of both amino groups on the pyrimidine ring of PYR and the 6-ethyl side chain in the binding of the molecule to the Hex isozymes, consistent with the predictions derived from the crystal structure of the Hex B:PYR complex. We have demonstrated that, while the phenyl group and its associated moieties do not have a great impact on Hex binding, they significantly increase the ability of the derivatives to enhance the intracellular/

DOI: 10.1021/jm5017895
J. Med. Chem. 2015, 58, 4483−4493

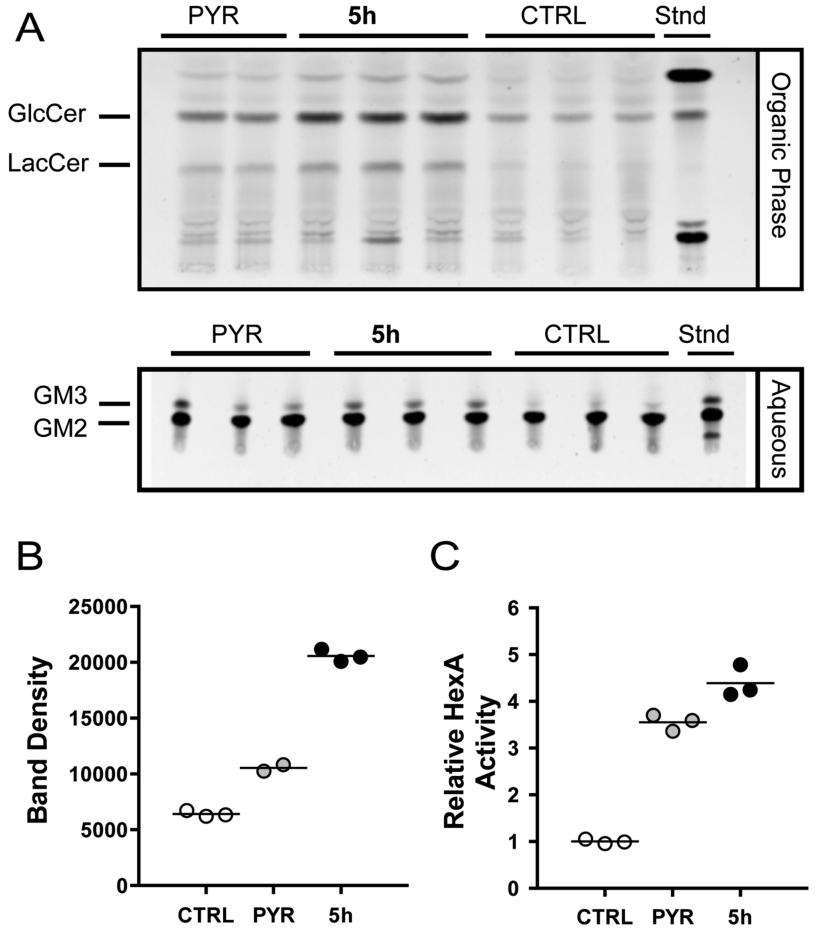

Figure 6. Increased intracellular hydrolysis of a fluorescent derivative of GM2 ganglioside in ATSD patient fibroblasts treated with **5h** or PYR. Hydrolyzed fluorescent GM2 ganglioside derivatives isolated from patient fibroblasts pre-loaded with fluorescent GM2 were resolved by TLC. (A) Chromatograms showing the resolution of metabolized GM2 derivatives in the two phases generated by Folch extraction. (B) Quantification of hydrolyzed levels of ganglioside was derived from the optical density of the bands corresponding to GM3 in the aqueous phase and LacCer and GlcCer in the organic phase. (C) Relative Hex A activity (MUGS) in lysates prepared from the cells used to measure GM2 hydrolysis following treatment with DMSO (Ctrl), PYR, or **5h**.

lysosomal activity of mutant G269S Hex A. We have identified a PYR derivative, **5h**, that further increases mutant Hex A activity by another 30% over the maximum observed with PYR. Significantly, we see an increase in the intracellular hydrolysis of GM2 in the lysosomes of fibroblasts treated with this compound. The maximal increase with **5h** is seen at a higher concentration than with PYR, which is likely caused by the more pronounced negative effects on cellular viability observed with PYR at concentrations >100 μM. As opposed to changes to the amino groups and ethyl arm on the pyrimidine ring, modifications to the phenyl group do not dramatically change the strength of binding, they but appear to decrease the toxicity and thus increase the apparent chaperoning efficacy of the compounds at higher concentrations. As a starting point, modification of the phenyl headgroup represents a site for making further improvements in chaperoning efficacy while minimizing toxicity.

EXPERIMENTAL SECTION

Experimental Protocols—Chemistry. Unless otherwise stated, ^{1}H (300 MHz) and ^{13}C (75.5 MHz) NMR spectra were recorded at room temperature (rt). Chemical shifts are reported in parts per million (ppm) on the δ scale, and coupling constants, J, are given in hertz (Hz). Multiplicities are reported as "s" (singlet), "d" (doublet), "t" (triplet), "q" (quartet), "dd" (doublet of doublets), "ddd" (doublet of doublets of doublets), and "m" (multiplet), and further qualified as "br" (broad) or "c" (complex). Infrared (IR) spectra (cm^{-1}) were recorded from films deposited on NaCl plates. Mass spectra (m/z) were recorded in the electrospray ionization (ESI) or atmospheric pressure chemical ionization (APCI) mode, as indicated. Melting points (mp, uncorrected) were measured on a Mel-Temp apparatus. Commercial reagents and solvents were used without further purification, except for THF (freshly distilled from Na/Ph_2CO under Ar) and CH_2Cl_2 (freshly distilled from CaH_2 under Ar). Commercial BuLi solutions were titrated against $Ph_2CHCOOH$.[20] The reactions were monitored by thin-layer chromatography (TLC) using silica gel 60 F_{254} pre-coated plates, and spots were visualized with a UV lamp or by using $KMnO_4$ or vanillin stain. Flash chromatography was performed on Silicycle 230–400 mesh silica gel. All reactions were carried out under an Ar atmosphere. Oven-dried flasks fitted with rubber septa for the introduction of substrates/reagents/solvents via syringe, and equipped with Teflon stirring bars, were employed for reactions involving air- and moisture-sensitive reagents.

General Procedure for the Preparation of Pyrimidine-2,4-diamines. A mixture of an appropriate 2-aryl-3-methoxy-3-alkyl-acrylonitrile[10] (4 mmol), guanidine hydrochloride (2 equiv), and $NaHCO_3$ (2.2 equiv) in dry DMSO (10 mL) was heated at 90 °C for **5h**. The cooled mixture was poured into EtOAc and washed sequentially with water, saturated $NaHCO_3$ solution, and brine. The organic phase was dried ($MgSO_4$) and concentrated under reduced pressure. The crude product was purified by trituration with diethyl

DOI: 10.1021/jm5017895
J. Med. Chem. 2015, 58, 4483–4493

ether/hexanes or by recrystallization from methanol/diethyl ether. Overall yields were between 20 and 30% and were not further optimized unless the compound proved to be of interest. The following compounds were thus obtained:

*5-(4-Chlorophenyl)-6-methylpyrimidine-2,4-diamine (**5a**).* Known compound,[21] mp >260 °C (lit.[18] 264−265 °C). IR: 3471, 3306, 3091, 1624, 1553, 1477 1438, 1263, 1086. ^{1}H NMR (acetone-d_6): 7.45 (2H, d, J = 8.3, ArH), 7.26 (2H, d, J = 8.3, ArH), 5.38 (2H, bs, NH_2), 5.26 (2H, bs, NH_2), 1.89 (3H, s, Me). ^{13}C NMR (DMSO-d_6): 162.4 (C), 162.3 (C), 162.2 (C), 135.6 (C), 132.9 (CH), 132.1 (C), 129.3 (CH), 106.2 (C), 22.4 (Me). APCI-MS: 235.3 $[M^{35}Cl+H]^+$ (100%) and 237.2 $[M^{37}Cl+H]^+$ (35%).

*5-(4-Chlorophenyl)-6-propylpyrimidine-2,4-diamine (**5b**).* Known compound,[22] mp 173−175 °C (lit.[21] 171−174 °C). IR: 3456, 3309, 3162, 2965, 1627, 1549, 1428, 1401, 1273, 1088, 1000. ^{1}H NMR ($CDCl_3$): 7.44 (2H, d, J = 8.5, ArH), 7.18 (2H, d, J = 8.5, ArH), 5.18 (2H, bs, NH_2), 4.61 (2H, bs, NH_2), 2.26 (2H, t, J = 7.8, $C\underline{H_2}CH_2Me$), 1.55 (2H, sex, J = 7.8, $CH_2C\underline{H_2}Me$), 0.81 (3H, t, J = 7.4, $CH_2CH_2\underline{Me}$). ^{13}C NMR (DMSO-d_6): 165.2 (C), 162.14 (C), 162.11 (C), 135.2 (C), 132.8 (CH), 131.9 (C), 129.0 (CH), 105.9 (C), 36.2 (CH_2), 21.6 (CH_2), 14.1 (Me). ESI-MS: 263.2 $[M^{35}Cl+H]$ (100%) and 265.1 $[M^{35}Cl+H]^+$ (35%).

*5-(4-Chlorophenyl)-6-isopropylpyrimidine-2,4-diamine (**5c**).* Mp 240−242 °C. IR: 3440, 3317, 3126, 2967, 1628, 1549, 1425, 1275, 1248, 1086. ^{1}H NMR ($CDCl_3$): 7.43 (2H, d, J = 8.4, ArH), 7.18 (2H, d, J = 8.4, ArH), 4.74 (2H, bs, NH_2), 4.40 (2H, bs, NH_2), 2.63 (1H, sept, J = 6.7, $C\underline{H}(Me)_2$, 1.07 (6H, d, J = 6.7, $CH(\underline{Me})_2$. ^{13}C NMR ($CDCl_3$): 172.2 (C), 162.1 (C), 161.9 (C), 134.0 (C), 133.8 (C), 132.0 (CH), 129.5 (CH), 106.6 (C), 31.1 (CH), 21.4 (Me). APCI-MS: 263.4 $[M^{35}Cl+H]^+$ (100%) and 265.3 $[M^{35}Cl+H]^+$ (35%). ESI-HRMS: calcd for $C_{13}H_{16}N_4{}^{35}Cl$ $[M+H]^+$ 263.1063; found 263.1061.

*5-(4-Chlorophenyl)-6-butylpyrimidine-2,4-diamine (**5d**).* Known compound,[21] mp 204−207 °C (lit.[21] 208−210 °C). ^{1}H NMR (DMSO-d_6): 7.45 (2H, app d, J = 8.3, ArH), 7.16 (2H, app d, J = 8.3, ArH), 5.98 (2H, bs, NH_2), 5.70 (2H, bs, NH_2), 2.10−2.05 (2H, cm, Ar-$\underline{CH_2}(CH_2)_2CH_3$), 1.39 (2H, quintet, J = 7.4, Ar-$CH_2\underline{CH_2}CH_2CH_3$), 1.10 (2H, sextet, J = 7.4, $Ar(CH_2)_2\underline{CH_2}CH_3$), 0.70 (3H, t, J = 7.4, $Ar(CH_2)_3\underline{CH_3}$). ^{13}C NMR (DMSO-$d_6$): 165.0 (C), 162.6 (C), 162.0 (C), 135.2 (C), 133.1 (CH), 132.3 (C), 129.3 (CH), 106.3 (C), 33.9 (CH_2), 30.8 (CH_2), 22.4 (CH_2), 14.1 (Me).

*6-(Aminomethyl)-5-(4-chlorophenyl)pyrimidine-2,4-diamine (**5e**).* Treatment of 5-(4-chlorophenyl)-6-benzyloxymethyl-pyrimidine-2,4-diamine (prepared by the general procedure above from benzyloxyacetyl chloride and 2-(4-chlorophenyl)acetonitrile) with 45% HBr in AcOH[23] afforded 5-(4-chlorophenyl)-6-bromomethyl-pyrimidine-2,4-diamine, which was purified by trituration with ether. A portion of this material (32 mg, 102 mmol) was reacted with NaN_3 (66 mg, 1.02 mmol, 10 equiv) in DMSO (5 mL, rt, 12 h). The customary aqueous extractive workup afforded a solid, which was triturated with ether to afford 11 mg (30%) of pure **5e**, mp 155−158 °C. IR: 3459, 3320, 3168, 2922, 2101, 1623, 1551, 1435, 1260, 1089, 1009. ^{1}H NMR ($CDCl_3$): 7.45 (2H, d, J = 8.0, ArH), 7.20 (2H, d, J = 8.0, ArH), 5.0 (2H, bs, NH_2), 4.73 (2H, bs, NH_2), 3.88 (2H, s, CH_2). ^{13}C NMR ($CDCl_3$): 162.5 (C), 161.9 (C), 160.1 (C), 134.6 (C), 133.9 (C), 131.8 (CH), 129.8 (CH), 107.7 (C), 52.1 (CH_2). APCI-MS: 276.4 $[M^{35}Cl+H]^+$ (100%) and 278.3 $[M^{37}Cl+H]^+$ (30%). ESI-HRMS: calcd for $C_{11}H_{11}N_7{}^{35}Cl$ $[M+H]^+$ 276.0764; found 276.0764.

Zinc dust (78 mg, 1.2 mmol) was added to a solution of the above azido compound (11 mg, 40 mmol) in THF/$NH_4Cl_{(aq)}$ (2 mL, 1:1) and stirred at rt for 1 h. The solution was filtered through Celite, diluted with water, and extracted with ethyl acetate. The combined organic extracts were dried (Na_2SO_4) and concentrated under reduced pressure. The crude residue was triturated with chloroform to the give the product as a colorless solid (10 mg, 100%), mp 171−174 °C. IR: 3331, 3206, 2920, 1612, 1546, 1455, 1348, 1257, 1088, 1007.^{1}H NMR (acetone-d_6): 7.55 (2H, d, J = 8.2, ArH), 7.43 (2H, d, J = 8.2, ArH), 6.14 (2H, bs, NH_2), 4.35 (2H, s, CH_2). ^{13}C NMR (acetone-d_6): 163.8 (C), 160.5 (C), 157.3 (C), 134.0 (C), 132.4 (CH), 131.2 (C), 129.8 (CH), 105.8 (C), 51.3 (CH_2). APCI-MS 250.5 $[M^{35}Cl+H]^+$ (100%) and 252.4 $[M^{37}Cl+H]^+$ (100%). ESI-HRMS: calcd for $C_{11}H_{13}N_5{}^{35}Cl$ $[M+H]^+$ 250.0859; found 250.0858.

*6-Ethyl-5-(4-(methoxyphenyl)pyrimidine-2,4-diamine (**5f**).* ^{1}H NMR (DMSO-d_6): 7.49 (2H, d, J = 8.4, ArH), 6.98 (2H, d, J = 8.4, ArH), 5.81 (2H, bs, NH_2), 5.40 (2H, bs, NH_2), 3.78 (3H, s, OCH_3), 2.10 (2H, q, J = 7.0, CH_2), 0.95 (3H, t, J = 7.0, CH_3). ^{13}C NMR (DMSO-d_6): 167.1 (C), 162.8 (C), 162.4 (C), 158.7 (C), 132.1 (CH), 128.2 (C), 114.8 (CH), 108.5 (C), 55.4 (CH_3), 27.9 (CH), 13.6 (Me).

*6-Ethyl-5-(4-(trifluoromethyl)phenyl)pyrimidine-2,4-diamine (**5g**).* Known compound,[24] mp 194−197 °C (lit.[22] mp not given). IR: 3499, 3316, 3167, 1625, 1554, 1441, 1314, 1123, 1101, 1013; ^{1}H NMR ($CDCl_3$): 7.71 (2H, d, J = 8.0, ArH), 7.39 (2H, d, J = 8.0, ArH), 4.99 (2H, bs, NH_2), 4.58 (2H, bs, NH_2), 2.26 (2H, q, J = 7.6, $C\underline{H_2}Me$), 1.07 (3H, t, J = 7.6, $CH_2\underline{Me}$). ^{13}C NMR ($CDCl_3$): 168.6 (C), 162.0 (C), 161.8 (C), 139.5 (C), 131.1 (CH), 130.0 (q, J_{C-F} = 32.7, C), 126.2 (q, J_{C-F} = 3.7, CH), 124.0 (q, J_{C-F} = 272.1, CF_3), 107.1 (C), 28.2 (CH_2), 13.3 (Me). APCI-MS: 283.4 $[M+H]^+$ (100%).

*6-Ethyl-5-phenylpyrimidine-2,4-diamine (**5h**).* Known compound,[21] optimized yield 86%, mp 242−244 °C (lit.[21] 237−240 °C). IR: 3423, 3301, 3152, 2980, 1628, 1556, 1430, 1273, 1230, 1069. ^{1}H NMR ($CDCl_3$): 7.48−7.23 (5H, m, ArH), 4.70 (2H, bs, NH_2), 4.45 (2H, bs, NH_2), 2.30 (2H, q, J = 7.6, $C\underline{H_2}Me$), 1.07 (3H, t, J = 7.6, $CH_2\underline{Me}$). ^{13}C NMR (DMSO-d_6): 166.9 (C), 162.5 (C), 136.4 (C), 131.0 (CH), 129.4 (CH), 127.6 (CH), 107.0 (C), 27.9 (CH_2), 13.6 (Me). ESI-MS: 215.4 (M+H, 100%).

*6-Ethyl-5-(p-tolyl)pyrimidine-2,4-diamine (**5i**).* Mp 212−215 °C. IR: 3305, 1627, 1567, 1233. ^{1}H NMR (DMSO): 7.24 (d, 2H, J = 7.9 Hz), 7.06 (d, 2H, J = 7.9 Hz), 6.25 (s, 2H), 5.90 (b.s, 2H), 2.33 (s, 3H), 2.11 (q, 2H, J = 7.6 Hz), 0.96 (t, 3H, J = 7.6 Hz). ^{13}C NMR ($CDCl_3$): 168.0, 162.4, 161.3, 137.6, 130.3, 129.9, 108.3, 28.0, 21.2, 13.4. LRMS: 229.4 $[M+H^+]$. HRMS: calcd for $C_{13}H_{17}N_4$ 229.1453; found $[M+H^+]$.

*6-Ethyl-5-(m-tolyl)pyrimidine-2,4-diamine (**5j**).* Mp 200−202 °C. IR: 3423, 3302, 3144, 2974, 1624, 1556, 1433, 1280, 1232, 1124, 1002. ^{1}H NMR (DMSO-d_6) 7.30 (1H, t, J = 7.6, ArH), 7.13 (1H, d, J = 7.6, ArH), 6.98 (1H, s, ArH), 6.95 (1H, d, J = 7.6, ArH), 5.82 (2H, bs, NH_2), 5.39 (2H, bs, NH_2), 2.31 (3H, s, Me), 2.09 (2H, q, J = 7.5, $C\underline{H_2}Me$), 0.94 (3H, t, J = 7.5, $CH_2\underline{Me}$). ^{13}C NMR ($CDCl_3$): 168.4 (C), 162.2 (C), 161.7 (C), 138.9 (C), 135.2 (C), 131.1 (CH), 129.0 (CH), 128.5 (CH), 127.5 (CH), 108.6 (C), 28.2 (CH_2), 21.4 (Me), 13.4 (Me). APCI-MS: 229.3 $[M+H]^+$ (100%). ESI-HRMS: calcd for $C_{13}H_{17}N_4$ $[M+H]^+$ 229.1453; found 229.1451.

*6-Ethyl-5-(o-tolyl)pyrimidine-2,4-diamine (**5k**).* Mp 174−176 °C. IR: 3439, 3311, 3175, 2977, 1624, 1549, 1428, 1267, 1113, 984. ^{1}H NMR ($CDCl_3$) 7.31−7.29 (3H, m, ArH), 7.13 (1H, d, J 8.1, ArH), 4.70 (2H, bs, NH_2), 4.34 (2H, bs, NH_2), 2.20 (2H, q, J = 7.6, $C\underline{H_2}Me$), 2.14 (3H, s, Me), 1.04 (3H, t, J = 7.6, $CH_2\underline{Me}$). ^{13}C NMR ($CDCl_3$): 168.4 (C), 161.89 (C), 161.86 (C), 137.9 (C), 134.2 (C), 131.0 (CH), 130.6 (CH), 128.3 (CH), 126.6 (CH), 107.4 (C), 28.1 (CH_2), 19.5 (Me), 12.8 (Me). APCI-MS: 229.4 $[M+H]^+$ (100%). ESI-HRMS: calcd for $C_{13}H_{17}N_4$ $[M+H]^+$ 229.1453; found 229.1455.

*5-(3,5-Dimethylphenyl)-6-ethylpyrimidine-2,4-diamine (**5l**).* Mp 223−225 °C. IR: 3405, 3310, 3169, 2971, 2922, 1600, 1553, 1430, 1276, 1003. ^{1}H NMR (DMSO-d_6): 6.94 (1H, s, ArH), 6.75 (2H, s, ArH), 5.79 (2H, bs, NH_2), 5.34 (2H, bs, NH_2), 2.27 (3H, s, Me), 2.09 (2H, q, J = 7.5, $C\underline{H_2}Me$), 0.94 (3H, t, J = 7.5, $CH_2\underline{Me}$). ^{13}C NMR ($CDCl_3$): 168.3 (C), 162.3 (C), 161.6 (C), 138.7 (C), 135.1 (C), 129.3 (CH), 128.1 (CH), 108.7 (C), 28.1 (CH_2), 21.3 (Me), 13.4 (Me). APCI-MS: 243.4 $[M+H]^+$ (100%). ESI-HRMS: calcd for $C_{14}H_{19}N_4$ $[M+H]^+$ 243.1610; found 243.1606.

*2-Amino-6-ethyl-5-(4-chlorophenyl)pyrimidin-4(3H)-one (**6**).* Known compound prepared as described by Trattner et al. in 1964.[25] This material was not purified and was advanced to **8** in crude form (<85% purity). ^{1}H NMR (DMSO-d_6): 7.77 (d, 2H, J = 8.2 Hz, ArH), 7.44 (d, 2H, J = 8.2 Hz, ArH), 7.0 (br s, 1H, NH), 5.8 (br s, 1H, NH), 3.35 (br s, 1H, NH), 2.04 (q, 2H, J = 7.5 Hz, CH_2), 1.02 (t, 3H, J = 7.5 Hz, CH_3). ^{13}C NMR (DMSO-d_6): 165.4 (C), 157.1 (C), 156.1 (C), 138.3 (C), 132.3 (CH), 126.3 (CH), 122.9 (C), 103.2 (C), 23.7 (CH_2), 13.4 (CH_3).

DOI: 10.1021/jm5017895
J. Med. Chem. 2015, 58, 4483−4493

*2-Amino-6-ethyl-5-(4-(trifluoromethyl)phenyl)pyrimidin-4(3H)-one (**7**).* ^{1}H NMR (DMSO-d_6): 7.68 (d, 2H, J = 8.0 Hz), 7.39 (d, 2H, J = 8.0 Hz), 6.67 (bs, 2H), 2.17 (q, 2H, J = 7.4 Hz), 1.02 (t, 3H, J = 7.4 Hz). ^{13}C NMR (DMSO-d_6): 162.7 (C), 155.0 (C), 140.6 (C), 132.0 (CH), 127.5 (q, J_{C-F} = 32 Hz, C), 126.7 (CH), 125.0 (q, J_{C-F} = 3.8 Hz, CH), 124.8 (q, J_{C-F} = 273 Hz, CF_3), 112.3 (C), 28.2 (CH_2), 13.3 (CH_3). IR: 3326, 3125, 1657, 1323. LRMS: [M+H$^+$] 284.4. HRMS: calcd for 284.1011 $C_{13}H_{13}F_3N_3O$; found 284.1021 [M+H$^+$].

*2-Amino-4-ethyl-5-(4-chlorophenyl)pyrimidine (**8**).* Known compound prepared as described by Russell et al. in 1954.[26] ^{1}H NMR ($CDCl_3$): 8.52 (s, 1H, Pyr-H), 7.49 (d, 2H, J = 8.1 Hz, ArH), 7.22 (d, 2H, J = 8.1 Hz, ArH), 4.79 (bs, 2H, NH_2), 2.41 (q, 2H, J = 7.5, $C\underline{H_2}Me$), 1.20 (t, 3H, J = 7.6, $CH_2\underline{Me}$). ^{13}C NMR ($CDCl_3$): 167.3 (C), 161.0 (C), 157.4 (C), 134.5 (C), 132.6 (C), 131.0 (CH), 129.9 (CH), 115.6 (C), 28.1 (CH_2), 13.3 (CH_3).

*2-Amino-4-ethyl-5-(4-(trifluoromethyl)phenyl)pyrimidine (**9**).* ^{1}H NMR ($CDCl_3$): 8.20 (s, 1H, Pyr-H), 7.74 (d, 2H, J = 8.0, ArH), 7.40 (d, 2H, J = 8.0, ArH), 6.35 (bs, 2H, NH_2) 2.72 (q, 2H, J = 7.5, $C\underline{H_2}Me$), 1.27 (t, 3H, J = 7.6, $CH_2\underline{Me}$). ^{13}C NMR (DMSO-d_6): 170.0 (C), 159.0 (C), 156.7 (C), 138.2 (C), 130.6 (q, J = 32 Hz, C), 129.7 (CH), 126.0 (q, J = 3.7 Hz, CH), 123.8 (q, J = 272 Hz, CF_3), 123.6 (C), 27.6 (CH_2), 12.7 (CH_3). IR: 3328, 3184, 1322. LRMS: 268.4 [M+H$^+$]. HRMS: calcd for $C_{13}H_{13}F_3N_3$ [M+H$^+$] 268.1056; found 268.1062 [M+H$^+$].

*4-Amino-6-ethyl-5-(4-(trifluoromethyl)phenyl)pyrimidin-2(1H)-one (**10**).* ^{1}H NMR (DMSO-d_6): 7.77 (d, 2H, J = 8.0 Hz), 7.43 (d, 2H, J = 8.0 Hz), 7.06 (bs, 1H), 5.85 (bs, 1H), 2.03 (q, 2H, J = 7.6 Hz), 0.94 (t, 3H, J = 7.4 Hz). ^{13}C NMR (DMSO-d_6): 165.2, 156.8, 156.2, 138.1, 132.3, 128.6 (q, J_{C-F} = 32 Hz, C), 126.3 (q, J_{C-F} = 3.8 Hz, CH), 124.8 (J_{C-F} = 273.1 Hz, CF_3), 103.2, 23.8 (CH_2), 13.4 (CH_3). IR: 3393, 1619, 1324. LRMS: 284.4 [M+H$^+$]. HRMS: calcd for $C_{13}H_{13}F_3N_3O$ [M+H$^+$] 284.1011; found 284.1013.

*4-Ethyl-5-(4-(trifluoromethyl)phenyl)pyrimidine (**11**).* ^{1}H NMR (DMSO-d_6): 9.16 (1H, s, Pyr-H), 8.63 (1H, s, Pyr-H), 7.88 (2H, app d, J = 8.0, ArH), 7.69 (2H, app d, J = 8.0, ArH), 2.71 (2H, q, J = 7.5, $C\underline{H_2}Me$), 1.15 (3H, t, J = 7.5, $CH_2\underline{Me}$). ^{13}C NMR (DMSO-d_6): 167.9 (C), 157.7 (C), 156.3 (C), 139.8 (C), 132.8 (C), 130.2 (CH), 128.8 (q, J_{C-F} = 32.0, C), 125.6 (q, J_{C-F} = 3.7, CH), 124.3 (q, J_{C-F} = 272.9, CF_3), 27.6 (CH_2), 12.3 (CH_3). IR: 3060, 2929, 2856, 1324 (v. strong). ESI-MS: 253 [M+H]$^+$ (100%). ESI-HRMS: calcd for $C_{13}H_{12}N_2F_3$ [M+H]$^+$ 253.0953; found 253.0954.

Monitoring Inhibitory Activity of PYR Derivatives against Hex A and Other Enzymes. All test compounds were dissolved in DMSO. For enzyme reactions, the compounds were diluted such that the concentration of the diluent was 1% DMSO. Inhibitory activity of the compounds was monitored using purified human Hex A isozyme isolated from human placenta,[27] together with the artificial substrate pNPGlcNAc. Enzyme reactions were performed at 37 °C in McIlvaine citrate phosphate buffer pH 4.5, containing 0.025% human serum albumin, using 10 ng/mL of human Hex A, one of the diluted compounds, and 1.6 mM colorimetric substrate pNPGlcNAc. Reactions were stopped with 0.1 M 2-amino-2-methyl-1 propanol (MAP) pH 10.5, and the absorbance was read in a Molecular Devices M2 spectrofluorometer with absorbance set to 405 nm. IC_{50} values were extracted from the dose−response curve following non-linear curve fitting according to a built-in function within Prism Graphpad 5.0. Analysis of the inhibitory activity of compounds against mutant or wild-type human Hex A or wild-type human Hex B was performed using the Hex isozymes isolated and enriched from the lysates of either unaffected or ATSD patient fibroblasts by DEAE ion exchange chromatography. Alternatively, affinity-purified Hex B or Hex A from human placenta was used for the assay.[28] IC_{50} values comparing the inhibitory activity of PYR versus its derivatives for the different mutant or wild-type Hex isozymes were determined and analyzed as described above, except that the fluorescent substrate 4-methylumbelliferyl-2-acetamido-2-deoxy-β-D-glucopyranoside (MUG, 1.6 mM), which is recognized by both the α- and β-active sites of the Hex isozymes, was used. Evaluation of the inhibitory activity of the compounds at neutral pH was performed as described above, except that pH 7 McIlvaine buffer was utilized. Inhibition studies requiring human DHFR were performed using bacterially expressed and purified human DHFR, supplied as a kit from Sigma-Aldrich (USA). Inhibition studies of purified human O-GlcNAcase by PYR were performed in the laboratory of Dr. David Vocadlo at Simon Fraser University (Burnaby, British Columbia, Canada) as described previously.[13]

Evaluating Intracellular Hex A Activity in Treated Patient Fibroblasts. The chaperoning efficacy of each PYR derivative, i.e., the maximum level of increase in mutant Hex A activity in treated versus non-treated fibroblasts from an ATSD patient, homozygous for the G269S mutation in the Hex α-subunit, was determined for each test compound. G269S cells were plated at 70−90% confluence (10 000−20 000 cells) in 96-well plates. Patient cells were treated for 5 days in the growth media (DMEM media supplemented with 10% fetal bovine serum) containing each of the PYR derivatives, serially diluted. DMSO levels were maintained at 1%. Subsequently, the media containing compounds were completely aspirated, and cells were washed twice with PBS prior to lysis of cells in McIlvaine buffer (pH 4.5), containing 0.4% Triton X-100 and 0.025% human serum albumin at 4 °C for 30 min. Aliquots of the crude lysates were used to measure Hex A and β-galactosidase activity utilizing the fluorogenic substrates, i.e., MU-2-acetamido-2-deoxy-β-D-glucopyranoside-6-sulfate (MUGS, 1.6 mM), which is hydrolyzed primarily by the α-active site of Hex A, and MU-β-galactopyranoside (0.45 mM), respectively. Enzyme reactions were performed at 37 °C for 1−2 h and subsequently terminated using 0.1 M MAP (pH 10.5) followed by fluorescence measurement (Ex = 365 nm and Em = 450 nm) on a Molecular Devices M2 spectrofluorometer. Intracellular enzyme activity levels were expressed relative to mock (1% DMSO) treated cells, where 1 = no change. All treatments were performed in triplicate.

Western Blotting and Immunofluorescence Imaging of Treated Patient Fibroblasts. Both methodologies were as previously described.[29] For immunofluorescence, fibroblasts were first fixed with 2.5% paraformaldehyde in PBS, permeabilized with 0.5% saponin, and blocked with 10% normal goat serum. The cells were then probed with a proprietary Hex A rabbit antibody, which was pre-absorbed with purified human Hex B to produce an α-specific antibody, and a LAMP1 mouse antibody (from the Developmental Studies Hybridoma Bank developed under the auspices of the NICHD and maintained by the University of Iowa, Department of Biological Sciences, Iowa City, IA 52242). Primary antibody binding was visualized using the corresponding secondary antibodies Alexa Fluor 488 anti-rabbit IgG (green) and Alexa Fluor 594 anti-mouse IgG (red) (Invitrogen) in the blocking solution.

Intracellular Hydrolysis of Fluorescent Analogues of GM2 Ganglioside. Intracellular hydrolysis of GM2 ganglioside was monitored using a fluorescent analogue of GM2 ganglioside (kindly provided by W. Wakarchuk, U. Ryerson, Toronto, Canada) as previously described.[8] ATSD patient fibroblasts (three confluent 10 cm plates) were treated with either PYR or one of its derivatives for 10 days. Prior to evaluation of the GM2 hydrolysis of the cell's endogenous mutant lysosomal Hex A, the cells were treated with conduritol β-epoxide (CBE, an irreversible glucocerebrosidase inhibitor) to limit hydrolysis beyond GlcCer and loaded with a fluorescent derivative of GM2 ganglioside for 8 h. Neutral glycolipids and gangliosides were separated by Folch extraction[30] of the treated cells and divided into two pools consisting of gangliosides in the aqueous layer and neutral glycolipids in the organic layer. Gangliosides and glycolipids were resolved by high-performance thin-layer chromatography and visualized/quantified by fluorescence imaging (Storm Imager, Molecular Devices).

■ ASSOCIATED CONTENT

Ⓢ Supporting Information

Figure S1, comparison of *in cellulo* enhancement of wild-type Hex A enzyme activity in fibroblasts treated with either DMSO, PYR, or **5h** (n = 4); spectral data and NMR spectra for representative compounds. The Supporting Information is available free of charge on the ACS Publications website at DOI: 10.1021/jm5017895.

DOI: 10.1021/jm5017895
J. Med. Chem. 2015, 58, 4483−4493

AUTHOR INFORMATION

Corresponding Author

*Phone: (416) 813-6161. E-mail: hex@sickkids.ca.

Author Contributions

The manuscript was written through contributions of all authors. All authors have given approval to the final version of the manuscript.

Notes

The authors declare no competing financial interest.

ACKNOWLEDGMENTS

Funds from CIHR "Team" grant (CTP-82944; M.C., M.B.T and D.M.) were used to support the research presented in the manuscript along with a kind donation from the Uger estate (D.M.). We are grateful for the fluorescent GM2 ganglioside derivative kindly synthesized by Warren Wakarchuk (Ryerson University, Ontario, CAN). We thank Kam S. Ho for helping with the preparations of compounds **5h**−**5l**. We also thank Dr. Brian Mark (University of Manitoba, Manitoba, CAN) for his helpful discussions and suggestions, particularly with regard to Figure 1B.

ABBREVIATIONS USED

PC, pharmacological chaperone; MU, 4-methylumbelliferyl; PYR, pyrimethamine; ATSD, adult-onset Tay-Sachs disease; ASD, adult-onset Sandhoff disease

REFERENCES

(1) Kongsaeree, P.; Khongsuk, P.; Leartsakulpanich, U.; Chitnumsub, P.; Tarnchompoo, B.; Walkinshaw, M. D.; Yuthavong, Y. Crystal structure of dihydrofolate reductase from Plasmodium vivax: pyrimethamine displacement linked with mutation-induced resistance. *Proc. Natl. Acad. Sci. U.S.A.* **2005**, *102*, 13046−13051.

(2) Maegawa, G. H.; Tropak, M.; Buttner, J.; Stockley, T.; Kok, F.; Clarke, J. T.; Mahuran, D. J. Pyrimethamine as a potential pharmacological chaperone for late-onset forms of GM2 gangliosidosis. *J. Biol. Chem.* **2007**, *282*, 9150−9161.

(3) Clarke, J. T.; Mahuran, D. J.; Sathe, S.; Kolodny, E. H.; Rigat, B. A.; Raiman, J. A.; Tropak, M. B. An open-label Phase I/II clinical trial of pyrimethamine for the treatment of patients affected with chronic GM2 gangliosidosis (Tay-Sachs or Sandhoff variants). *Mol. Genet. Metab.* **2011**, *102*, 6−12.

(4) Knight, E. M.; Williams, H. N.; Stevens, A. C.; Kim, S. H.; Kottwitz, J. C.; Morant, A. D.; Steele, J. W.; Klein, W. L.; Yanagisawa, K.; Boyd, R. E.; Lockhart, D. J.; Sjoberg, E. R.; Ehrlich, M. E.; Wustman, B. A.; Gandy, S. Evidence that small molecule enhancement of beta-hexosaminidase activity corrects the behavioral phenotype in Dutch APP mice through reduction of ganglioside-bound Abeta. *Mol. Psych.* **2014**, *20*, 109−117.

(5) Sandhoff, K.; Harzer, K. Gangliosides and gangliosidoses: principles of molecular and metabolic pathogenesis. *J. Neurosci.* **2013**, *33*, 10195−10208.

(6) Mahuran, D. J. Biochemical consequences of mutations causing the GM2 gangliosidoses. *Biochim. Biophys. Acta* **1999**, *1455*, 105−138.

(7) Leinekugel, P.; Michel, S.; Conzelmann, E.; Sandhoff, K. Quantitative correlation between the residual activity of beta-hexosaminidase A and arylsulfatase A and the severity of the resulting lysosomal storage disease. *Hum. Genet.* **1992**, *88*, 513−23.

(8) Tropak, M. B.; Bukovac, S. W.; Rigat, B. A.; Yonekawa, S.; Wakarchuk, W.; Mahuran, D. J. A sensitive fluorescence-based assay for monitoring GM2 ganglioside hydrolysis in live patient cells and their lysates. *Glycobiology* **2010**, *20*, 356−65.

(9) Bateman, K. S.; Cherney, M. M.; Mahuran, D. J.; Tropak, M.; James, M. N. Crystal structure of beta-hexosaminidase B in complex with pyrimethamine, a potential pharmacological chaperone. *J. Med. Chem.* **2011**, *54*, 1421−1429.

(10) Tarnchompoo, B.; Sirichaiwat, C.; Phupong, W.; Intaraudom, C.; Sirawaraporn, W.; Kamchonwongpaisan, S.; Vanichtanankul, J.; Thebtaranonth, Y.; Yuthavong, Y. Development of 2,4-diaminopyrimidines as antimalarials based on inhibition of the S108N and C59R +S108N mutants of dihydrofolate reductase from pyrimethamine-resistant Plasmodium falciparum. *J. Med. Chem.* **2002**, *45*, 1244−1252.

(11) Griffin, R. J.; Schwalbe, C. H.; Stevens, M. F. G.; Wong, K. P. Structural studies on bio-active compounds.III. Re-examination of the hydrolysis of the antimalarial drug pyrimethamine and related derivatives and crystal-structure of a hydrolysis product. *J. Chem. Soc., Perkin Trans. 1* **1985**, 2267−2276.

(12) Mark, B. L.; Mahuran, D. J.; Cherney, M. M.; Zhao, D.; Knapp, S.; James, M. N. Crystal structure of human beta-hexosaminidase B: understanding the molecular basis of Sandhoff and Tay-Sachs disease. *J. Mol. Biol.* **2003**, *327*, 1093−1109.

(13) Macauley, M. S.; Whitworth, G. E.; Debowski, A. W.; Chin, D.; Vocadlo, D. J. O-GlcNAcase uses substrate-assisted catalysis: kinetic analysis and development of highly selective mechanism-inspired inhibitors. *J. Biol. Chem.* **2005**, *280*, 25313−25322.

(14) Takakura, A.; Nelson, E. A.; Haque, N.; Humphreys, B. D.; Zandi-Nejad, K.; Frank, D. A.; Zhou, J. Pyrimethamine inhibits adult polycystic kidney disease by modulating STAT signaling pathways. *Hum. Mol. Genet.* **2011**, *20*, 4143−4154.

(15) Reich, N. C.; Liu, L. Tracking STAT nuclear traffic. *Nat. Rev. Immunol.* **2006**, *6*, 602−612.

(16) Horvath, C. M. STAT proteins and transcriptional responses to extracellular signals. *Trends Biochem. Sci.* **2000**, *25*, 496−502.

(17) Hasilik, A.; Neufeld, E. F. Biosynthesis of lysosomal enzymes in fibroblasts: synthesis as precursors of higher molecular weight. *J. Biol. Chem.* **1980**, *255*, 4937−4945.

(18) Weiss, L. M.; Harris, C.; Berger, M.; Tanowitz, H. B.; Wittner, M. Pyrimethamine concentrations in serum and cerebrospinal fluid during treatment of acute Toxoplasma encephalitis in patients with AIDS. *J. Infect. Dis.* **1988**, *157*, 580−583.

(19) Pajouhesh, H.; Lenz, G. R. Medicinal chemical properties of successful central nervous system drugs. *NeuroRx* **2005**, *2*, 541−553.

(20) Kofron, W. G.; Baclawski, L. M. Convenient method for estimation of alkyllithium concentrations. *J. Org. Chem.* **1976**, *41*, 1879−1880.

(21) Russell, P. B.; Hitchings, G. H. 2,4-diaminopyrimidines as antimalarials.III. 5-aryl derivatives. *J. Am. Chem. Soc.* **1951**, *73*, 3763−3770.

(22) Rogers, E. F.; Leanza, W. J.; Sarett, L. H. Antiparasitic agents 0.1. Some new 2,4-diaminopyrimidines. *J. Org. Chem.* **1957**, *22*, 1492−1494.

(23) Liu, B.; Liu, M.; Xin, Z. L.; Zhao, H. Y.; Serby, M. D.; Kosogof, C.; Nelson, L. T. J.; Szczepankiewicz, B. G.; Kaszubska, W.; Schaefer, V. G.; Falls, H. D.; Lin, C. W.; Collins, C. A.; Sham, H. L.; Liu, G. Optimization of 2,4-diaminopyrimidines as GHS-R antagonists: Side chain exploration. *Bioorg. Med. Chem. Lett.* **2006**, *16*, 1864−1868.

(24) Barlin, G. B.; Kotecka, B.; Rieckmann, K. H. Potential antimalarials.XXII. Some 2,4-diamino-5-(3- and 4-trifluoromethylphenyl and 3,4-methylenedioxyphenyl)pyrimidines. *Aus. J. Chem.* **1996**, *49*, 647−650.

(25) Trattner, R. B.; Hitchings, G. H.; Sharefkin, D. M.; Elion, G. B. Deamination studies on pyrimidine and condensed pyrimidine systems. *J. Org. Chem.* **1964**, *29*, 2674−2677.

(26) Russell, P. B. The effects of substitution on the ultra-violet absorption spectra of phenylpyrimidines. *J. Chem. Soc.* **1954**, 2951−2955.

(27) Mahuran, D.; Lowden, J. A. The subunit and polypeptide structure of hexosaminidases from human placenta. *Can. J. Biochem.* **1980**, *58*, 287−294.

(28) Tropak, M. B.; Reid, S. P.; Guiral, M.; Withers, S. G.; Mahuran, D. Pharmacological enhancement of beta-hexosaminidase activity in fibroblasts from adult Tay-Sachs and Sandhoff Patients. *J. Biol. Chem.* **2004**, *279*, 13478−13487.

DOI: 10.1021/jm5017895
J. Med. Chem. 2015, 58, 4483−4493

(29) Tropak, M. B.; Kornhaber, G. J.; Rigat, B. A.; Maegawa, G. H.; Buttner, J. D.; Blanchard, J. E.; Murphy, C.; Tuske, S. J.; Coales, S. J.; Hamuro, Y.; Brown, E. D.; Mahuran, D. J. Identification of pharmacological chaperones for Gaucher disease and characterization of their effects on beta-glucocerebrosidase by hydrogen/deuterium exchange mass spectrometry. *ChemBioChem* **2008**, *9*, 2650−2662.
(30) Lees, M.; Folch, J.; Stanley, G. H.; Carr, S. A simple procedure for the preparation of brain sulphatides. *J. Neurochem.* **1959**, *4*, 9−18.

DOI: 10.1021/jm5017895
J. Med. Chem. 2015, 58, 4483−4493